Tomas Bata University in Zlín
Library

The adsorption, kinetics, and interaction mechanisms of various types of estrogen on electrospun polymeric nanofiber membranes

Citation

YASIR, Muhammad, Tomáš ŠOPÍK, Lenka LOVECKÁ, Dušan KIMMER, and Vladimír SEDLAŘÍK. The adsorption, kinetics, and interaction mechanisms of various types of estrogen on electrospun polymeric nanofiber membranes. *Nanotechnology* [online]. vol. 33, iss. 7, IOP Publishing, 2022, [cit. 2023-03-31]. ISSN 0957-4484. Available at https://iopscience.iop.org/article/10.1088/1361-6528/ac357b

DOI

https://doi.org/10.1088/1361-6528/ac357b

Permanent link

https://publikace.k.utb.cz/handle/10563/1010677

This document is the Accepted Manuscipt version of the article that can be shared via institutional repository.

TBU Publications
Repository of TBU Publications
publikace.k.utb.cz

The adsorption, kinetics, and interaction mechanisms of various types of estrogen on electrospun polymeric nanofiber membranes

Muhammad Yasir*, Tomáš Šopík, Lenka Lovecká, Dušan Kimmer and Vladimír Sedlařík*

Centre of Polymer Systems, University Institute, Tomas Bata University in Zlín, Třída Tomáše Bati 5678, 760 01Zlín, Czech Republic

E-mail: yasir@utb.cz and sedlarik@utb.cz

Abstract

This study focuses on the adsorption kinetics of four highly potent sex hormones (estrone (E1), 17β-estradiol (E2), 17α-ethinylestradiol (EE2), and estriol (E3)), present in water reservoirs, which are considered a major cause of fish feminization, low sperm count in males, breast and ovarian cancer in females induced by hormonal imbalance. Herein, electrospun polymeric nanostructures were produced from cellulose acetate, polyamide, polyethersulfone, polyurethanes (918 and elastollan), and polyacrylonitrile (PAN) to simultaneously adsorbing these estrogenic hormones in a single step process and to compare their performance. These nanofibers possessed an average fiber diameter in the range 174-330 nm and their specific surface area ranged between 10.2 and 20.9 m^2 g^{-1}. The adsorption-desorption process was investigated in four cycles to determine the effective reusability of the adsorption systems. A one-step high-performance liquid chromatography technique was developed to detect and quantify concurrently each hormone present in the solution. Experimental data were obtained to determine the adsorption kinetics by applying pseudo-first-order, pseudo-second-order and intraparticle diffusion models. Findings showed that E1, E2 and EE2 best fitted pseudo-second-order kinetics, while E3 followed pseudo-first-order kinetics. It was found that polyurethane Elastollan nanofibers had maximum adsorption capacities of 0.801, 0.590, 0.736 and 0.382 mg g^{-1} for E1, E2, EE2 and E3, respectively. In addition, the results revealed that polyurethane Elastollan nanofibers had the highest percentage efficiency of estrogens removal at ∼58.9% due to its strong hydrogen bonding with estrogenic hormones, while the least removal efficiency for PAN at ∼35.1%. Consecutive adsorption-desorption cycles demonstrated that polyurethane maintained the best efficiency, even after being repeatedly used four times compared to the other polymers. Overall, the findings indicate that all the studied nanostructures have the potential to be effective adsorbents for concurrently eradicating such estrogens from the environment.

Keywords: wastewater treatment, estrogenic hormones, static adsorption, kinetics, electrospun, nanofibers

1. Introduction

Synthetic estrogenic hormones, also called endocrine-disrupting chemicals (EDCs), have an adverse effect on both human beings and animals **[1, 2]**. Residual micropollutants of this type are observed in low concentrations—at the level of micro-and nanograms—in cleaning reservoirs at wastewater treatment plants **[1]**. This problem has aroused serious concerns among the scientific community since synthetic hormones are known to interfere with the functional groups of natural hormones by blocking endogenous and mimic ability, which makes it much more dangerous **[3-7]**. The presence of estrogenic

hormones represents a severe threat to human and aquatic life through exposure via food sources or drinking water **[7, 8]**.

Estrogenic hormones include estrone (E1), estradiol (E2), ethinylestradiol (EE2) and estriol (E3), which disrupt the reproduction of aquatic species and the function of natural hormones in the human body **[8]**. Studies have proven that a rise in femininity occurs in fish, weight loss affects the testicles of quails and alligators experience issues with fertility **[9]**. Meanwhile, reports show that humans demonstrate a decline in the sperm counts of males and the risk of breast and ovarian cancer is heightened in females **[10]**. Quantities of these estrogenic hormones have been observed downstream of the treatment plants **[11-13]**, with lower limits having been reported of 3.4-41 ng l^{-1} at constructed wetlands in the Czech Republic **[14**]. Of the aforementioned estrogens, EE2 is a modern, formulated, synthetic estrogenic hormone used in oral contraceptive pills in the treatment of prostate cancer and menstrual problems in females **[15**]. It is considered the most fatal among all the estrogenic hormones as it only degrades partially at wastewater treatment plants and is challenging to be removed **[16]**. Consequently, the natural environment deconjugates the metabolites of EE2 and makes them active again under a suitable environment **[17]**. EE2 is the most potent EDC and is considered to have high estrogenicity **[18-20]**; hence, proper disposal of these estrogenic hormones is immediately required.

Conventional treatment plants cannot eliminate EDCs efficiently owing to their properties of low molecular weight and slow biodegradability **[21].** This has led to the widespread occurrence of the same quantity in reservoirs, rivers and lakes since they are released from treatment plants alongside treated effluents **[22, 23]**. In this regard, various strategies have been applied to capture, eliminate or completely degrade the EDCs and other common toxic chemical effluents, such as ozonation, membrane bioreactors, advanced oxidation, membrane filtration, coagulation, flocculation and photocatalysis **[24-26]**. Each technique has certain limitations, such as low efficiency and any resulting by-products demand further purification and sophisticated methods for processing them. Nano-filtration and reverse osmosis have proven to be interesting, but the extent of energy consumption makes them unfavorable for the treatment at a large scale **[27, 28]**.

In the context of the sorption technique, the choice of material selection is quite crucial. Adsorbent particles for estrogens have been reported, such as granules of activated charcoal **[29, 30]**, carbon nanomaterials **[31**], fullerene **[32**], carbon nanotubes **[33]**, chitosan, activated carbon, chitin, carbon-based adsorbents prepared from industrial waste **[34, 35**] and activated carbon fibers modified with iron hydroxide **[36]**. All of these are efficient, yet they require a process of additional separation from wastewater that raises the costs. Some researchers have recently found adsorbents such as nanofibers that could eradicate the need for a subsequent separation procedure **[37]**. To this end, not many studies have been reported. Therefore, it is necessary to test such high-performance materials with functionalized groups that can optimize the disposal process during the course of research programs.

Sorbents based on nanofibers have garnered much attention due to a number of favorable characteristics reported for them, such as large aspect ratio, high surface area and small pore size [**38]**. For this purpose, a versatile technique for generating continuous nanofibers is electrospinning, which gives rise to a material's diameter ranging from tens to hundreds of nanometers for adsorption and water filtration processes **[39, 40]**. The large aspect ratio of nanofibers gives significant rise to the filtration efficiency since the pore size is reduced; moreover, the large surface area allows greater contact between the solution and filtration-sorption adsorbent **[41]**. The apparatus requires an applied voltage between the cathode and anode to allow the electrostatic forces to overcome the tension on the surface of the polymer, thereby ejecting the polymeric solution and solidifying non-woven nanofibers on a collecting electrode covered in a textile substrate [**39, 42-45]**. The quality of nanofibers

can be improved by utilizing binary polymers with additives such as acetone and polyethylene oxide to obtain beadless nanostructures **[41].**

Past literature describes that electrospun polymers proved an excellent ability in removing heavy metal ions such as copper and organic pollutant dyes from wastewater **[46, 47].** However, fewer works have been done with electrospun polymers for estrogenic hormone removal applications. According to literature, research on commercially available nylon, polypropylene (PP), polytetrafluoroethylene, cellulose acetate, regenerated cellulose and glass microfiber filters have been reported for the removal of E1. Studies also report on polyamide (PA) nanoparticles being employed to extract just EE2. While polyethersulfone (PES) nanofibers for the removal of E2 and polyvinylidene fluoride (PVDF) doped with polyvinyl pyrrolidone (PVP) and titanium dioxide (TiO2) membranes prepared by phase inversion process for the removal of E1 and E2 have been reported. However, these studies have been solely limited to the filtration of single natural or synthetic hormones **[1, 15, 48, 49]**. This highlights the necessity of developing the least fiber diameter optimized nanofibers to extract such estrogenic hormones simultaneously and then gauge their kinetics for comparison **[50]**.

This paper primarily investigates the optimized preparation of electrospun nanostructures from polymers (cellulose- acetate (CA), polyurethanes (PU 918 and PU Elastollan), polyamide 6 (PA), polyethersulfone (PES) and polyacrylonitrile (PAN)) that possess beadless desired attributes of morphology, small diameter of the fiber, high ratio of surface area to volume, lightweight and numerous sites for adsorption. Research focuses on these nanostructured polymers with high sorption activity for estrogenic hormones (E1, E2, EE2 and E3). A membrane of this type could be employed for the microfiltration of wastewater compared to commercially available microfiltration membranes that exhibit greater flux **[45]**. The objective is simultaneous adsorption of four estrogenic hormones in a one-step process from wastewater at neutral pH because the pH of rivers is in the range of 6-9. The feasibility of the results is analyzed by applying experimental data, thereby determining adsorption capacity and kinetics via suitable models of pseudo-first-order, pseudo-second-order and intraparticle diffusion to help understand the suitability of characteristics essential for large scale implementation. Finally, the adsorption mechanisms of the nanofibers are gauged to understand the interaction ability of functional groups present for bonding between polymers and estrogenic hormones. The tests are conducted with the extent of polymers' reusability over several adsorption cycles to discern reliability and effectiveness for large scale generation of these polymers.

2. Materials and methods

2.1. Materials and reagents

The hormones under test (with purity in percent) comprised E1 $\geq$ 99%, E2 $\geq$ 98%, E3 $\geq$ 97% and EE2 $\geq$ 98% purchased from Sigma-Aldrich Chemie GmbH, Germany. Cellulose acetate CA-398-30 (CA) at the molar weight $M_w = 5 \times 10^4$ g mol^{-1} came from the Eastman Chemical Company, USA. Poly-urethane Elastollan EB_95A (PU Elastollan) at $M_w = 1.1 \times 10^5$ g mol^{-1} was bought from BASF Polyurethanes GmbH, Germany. Polyamide 6 (PA)— Silamid EN at $M_w = 1.45 \times 10^5$ g mol^{-1} was sourced from Roonamid a.s., Slovakia. Polyacrylonitrile PAN 181315 (PAN) of molecular weight $M_w = 1.5 \times 10^5$ g mol^{-1} was purchased from Sigma Aldrich, Germany. Polyethersulfone Ultrason E2020P SR (PES) at the molecular weight $M_w = 5.5 \times 10^4$ g mol^{-1} came from BASF SE, Germany. 4,4'-methylene-diphenyl diisocyanate (MDI), (poly 3-methyl-1,5-pentanediol-alt-adipic, isophthalic acid) (PAIM) and 1,4 butanediol (BD) were sourced from Sigma Aldrich, Germany. N,N-dimethylformamide (DMF >99.5%) was bought from Lach-Ner, s.r.o, Czech Republic. Acetic acid (AA (99%)), formic acid (FA (98%)), sodium tetra-borate decahydrate

(borax), citric acid, polyethylene oxide (PEO), dimethyla-mylamine (DMA) and 4-methyl-2-pentanone (MIBK) were purchased from PENTA s.r.o., Czech Republic.

Furthermore, HPLC solutions of acetonitrile (from Honeywell, Czech Republic) and ethanol (HPLC grade >99%; from VWR, Czech Republic) were utilized. Deionized water (pH 7.3, 18.2 Ω W cm^{-1}) was created on a laboratory Milli-*Q* ultrapure (Type 1) water purification system, Biopak® Polisher, Merck, USA and used throughout the study.

2.2. Preparation of the nanofibers

Each electrospun nanofiber was made from a different polymer; therefore, different solvents were used. A solution of the conductive components, borax and citric acid (BC), which was prepared at the ratio of 1:3, respectively and followed by 35 wt% of BC, was dissolved in DMF solution and stirred in a mixer for 5 h at 400 rpm to make it ready for adjusting the electrical conductivity of each treated solution prior to electrospinning. The synthesis of every electrospun material progressed under the optimized conditions and parameters required for that particular polymer as follows:

PA at the concentration of 18 wt% of the solution was dissolved in AA: FA at the ratio 2:1 for 4 h by stirring at 400 rpm in a mixer (Heidolph, RZR 2041) to homogenize the mixture uniformly. PU Elastollan 18 wt% was dissolved in DMF by treating the solution with BC to enhance electrical conductivity and optimize the electrospinning process. The solution of CA was prepared from 9% of powder in AA (57 wt%), ethanol (19 wt%), water (14.5 wt%) and PEO (0.3 wt%), followed by BC (0.2 wt%), which were stirred together to make a total of 400 g under constant stirring at 400 rpm for 6 h. PES solution (23 wt%) was prepared by dissolving the powder in 73 wt% DMA: MIBK at the ratio 3:1, supplemented by BC at 4 wt%. PAN powder was dissolved in DMF (9 wt%) under stirring for 5 h at 400 rpm. PU 918 was prepared via a polyaddition reaction at a centre of polymer systems (CPS) laboratory. PU solution in (DMF), based on MDI, PAIM polymer diol, $M_w = 2 \times 10^3$ g mol^{-1}) and BD was synthesized at the molar ratio 9:1:8 (PU 918) at 90 °C for 5 h per partes way of the synthesis, starting with the preparation of a pre-polymer from MDI and PAIM, followed by adding BD and the remaining quantity of MDI. After being supplemented with BC to idealize conductivity, the solution was electrospun at a concentration of 13 wt% PU with $M_w = 9.8 \times 10^4$ g mol^{-1} **[50]**.

The electrospinning process was performed in an electrostatic field on laboratory spin line equipment (CPS, Tomas Bata University, Czech Republic). The apparatus was equipped with a patented rotating electrode with three cotton cord spinning elements (PCT/CZ2010/000042) and a set of nanofiber-forming nozzles (jets) to produce fibers on polypropylene (PP) spun-bond non-woven textile of width 40 cm. The voltage applied was 75 kV during the electrospinning process, except for polyamide, when it equaled 130 kV. A set of 32 jet needles (2 rows of 16 each) was employed for the PU Elastollan, PES, PAN and PU 918; solution dosing was set to 0.34, 0.34, 0.13 and 0.24 ml min^{-1}, respectively, based on optimum parameters and conditions. The distance between the electrodes equaled 18 cm, apart from PU Elastollan, which equaled 19 cm. In the case of PA and CA, a solution was sprayed from the bath by cords set at 4 rpm, with the distance between the electrodes equaling 22 cm. The rotational speed of antistatic PP non-woven fabric was set at 10 cm min^{-1}, except for PA and PU 918, where the pace was set at 12 and 16 cm min^{-1}, respectively. The temperature was gauged as 28 ± 2 °C and relative air humidity was <35%. The solutions' electrical conductivity and intrinsic viscosity during preparation were maintained at optimal levels, as shown in **table 1**.

Table 1 shows the optimized properties of the polymeric solutions for subsequent electrospinning and the average mass per unit area of the resultant electrospun nanofibers. PA solution possessed the highest electrical conductivity, while the least was observed for CA. The concentration and intrinsic viscosity of the solutions varied between 9%-24% and 0.53-1.80 Pa.s, respectively. The value for average mass per unit area of the electrospun sheets was lowest for PU 918 and highest for PA. The given properties of solutions varied and set at optimum conditions to aim defect-free and beadless electrospun nanofibers.

Table 1. Properties of the polymeric solutions.

Sample	Concentration (%)	Density (g cm^{-3})	Intrinsic viscosity (Pa.s)	Electrical conductivity (μS cm^{-1})	Average mass per unit area (g m^{-2})
PES	24	1.350	0.75	102.0	1.02
PU 918	13	1.100	1.50	150.0	0.70
PU Elastollan	18	1.220	1.80	91.8	1.30
CA	9	1.315	1.64	83.4	1.63
PA	18	1.084	0.75	172.0	3.00
PAN	9	1.184	0.53	105.3	0.88

2.3. Characterization

Imaging on a Nova 450 scanning electron microscope (SEM) (FEI, Thermo Fisher Scientific, USA) was carried out to observe the morphology of the fiber surface, the desired diameter of the fiber and to check for defects such as beads in the structures at the acceleration voltage of 5-10 kV with a through-the-lens detector. A conductive gold coating (~120 s) was applied prior to examining the estrogenic hormones by a sputter coater. The mean fiber diameter of each polymer was determined using software ImageJ version 1.52a.

Fourier transformed infrared spectroscopy (FTIR) was performed on a Nicolet 320 spectrometer (ThermoScientific, USA) equipped with a Ge crystal to determine the functional groups of the polymeric nanofibers tested for adsorption of the estrogenic hormones. Attenuated total reflectance spectra were recorded across 400-4000 cm-1 under ambient temperature conditions, a scan rate of 16 and a resolution of 4 cm^{-1}.

Surface analysis of the nanofibers was carried out according to the Brunauer-Emmett-Teller (BET) method. A high-precision analyzer of surface area and pore size (BEL-SORP-mini II, BEL Japan Inc, Japan) was used to determine the specific surface area. Outgassing of the substrate occurred at 100 °C for 12 h in a vacuum prior to measurement.

The contact angle measurement was conducted by compressing the nanofibers to make them compact for accurate measurement. To this end, the nanofibers were put onto a single PP sheet that, in turn, was placed upside-down on a sheet of polyethylene terephthalate (PET). Subjected to a thermal press for 10 s at a temperature of 110 °C, then the layer of PP was detached. The sheet of PET with the nanofibers was covered with a glossy sheet for the thermal press, the same conditions being applied to acquire a smooth, compacted surface. This step ensured that liquid could remain on the surface for measuring the contact angles; without doing this, the surfaces of the nanofibers on the sheet of PP would have been incapable of holding the drops of liquid, which would instantly settle down, penetrating the porous structures. Finally, the contact angle of electrospun nanofibers was measured using the sessile drop technique on a goniometer (surface energy evaluation system (SEE System), Advex Instruments, Brno, Czech Republic) under the conditions of ambient temperature. A 5 µl pipette

dropped liquid onto the surface of the samples (10 x 10 mm^2), then the shapes of the resulting droplets were observed with the aid of a CCD camera and the contact angles measured immediately. Milli Q water was used as the probe liquid to determine the hydro-philicity **[51]**. The samples were analyzed and mean values for them are reported herein.

2.4. Solution preparation and sampling

A concentration of 0.2 mg l^{-1} of each hormone was prepared by adding 1 mg of the given hormone into 5 l of water; magnetic stirring was maintained at 800 rpm for 24 h to prepare 0.8 mg l^{-1} of solution and stored in the dark. Samples of 0.2, 0.15, 0.1, 0.05, 0.03 and 0.02 mg l^{-1} were collected by a micropipette (HTL Lab Solution, Poland) and dosed into 1.5 ml screw neck vials (VWR, Czech Republic) after passing through a glass microfiber (GMF) filter (Whatman, Czech Republic; of pore size 0.45 µm and 25 mm diameter). HPLC was performed on triplicated samples, resulting in mean concentrations plotted on a calibration curve.

2.5. High-performance liquid chromatography (HPLC)

The hormone samples (E1, E2, EE2, E3) were analyzed and their calibration standards were discerned on an HPLC Dio-nexUltiMate 3000 Series unit (Thermo Fisher Scientific, Germany). Separation took place on a reversed-phase column (Kinetex 2.6 µm C18 100 A, 150 x 4.6 mm; Phenomenex, USA) equipped with an ULTRA precolumn guard, UHPLC C18 (Phenomenex, USA) at 30 °C. A mixture of HPLC grade acetonitrile and water constituted the mobile phase (45:55, vol/vol) applied at the flow rate of 0.8 ml min^{-1} over a total isocratic run time of 12 min. The autosampler chamber was set to 5 °C and a volume of 20 µl was injected each time into the column. Eluates were detected at the wavelengths 200 and 205 nm and the concentration of hormones was calculated from the findings of the 200 nm tests (supplementary data, figure S1 (available online at **stacks.iop.org/NANO/33/ 075702/mmedia**)). A calibration vial with a concentration of 0.02 mg 1^{-1} was employed to determine the detection limit for each hormone; the limits equaled 1 µg 1^{-1} for E3, E2 and EE2 and 6 µg 1^{-1} for E1. Values for concentration were quantified by external calibration in software Chromeleon version 7.2 (Thermo Fisher Scientific, USA) **[52].**

2.6. Evaluation of the adsorption properties of polymeric nanofiber structure by discontinuous sorption testing

Static adsorption tests were carried out to determine the adsorption rate. Separate flasks were set aside for testing each polymeric mat in triplicates, utilizing 100 ml from the stock of estrogenic hormone solution at a total concentration of 0.8 mg 1^{-1}; each flask was then supplemented with 20 mg of a given nanofiber. The flasks were continuously stirred on an orbital incubator shaker (Stuart® S1500, Barloworld Scientific Ltd, UK) for adsorption at 250 rpm. Samples of the remaining concentration of the hormones in each flask were collected in vials via a 0.45 µm GMF syringe filter and readings were taken after intervals of 5 min, 15 min, 30 min, 60 min and each following hour until a constant value was obtained. At each interval, 4 ml samples were taken with a 20 ml syringe, ensuring that neither the nanofiber was removed nor destroyed in the process and 4 ml of ultrapure water was added to maintain total volume. The first 2 ml of the filtrate was discarded, this having passed from the syringe through the GMF filter to eliminate any adsorption during sampling, thereby ensuring accuracy and precision in the results. A flask containing a solution without any nanofiber was labeled

as ‘control’ and included in the experiment to discern the initial reference concentration. It must be noted that adsorption on the glass surface was negligible throughout long-term testing, which was determined by comparing the recorded initial concentration and concentration after 9 h of stirring the control solution. To this end, the hormone solutions were checked prior to the start of the experiment. Each sample reading was conducted in triplicate and the corresponding values for mean concentration and standard deviation based on Gaussian distribution were recorded. Finally, the percentage of adsorption for each hormone on the nanofibrous mat was calculated with reference to the aforementioned ‘control’ flask. The stock solution was kept neutral by means of ultrapure deionized water at a pH of 7.3, considering real environmental water samples to be in the range of 6-9. The percentage removed of each hormone at a given time (t) was determined by the expression in equation **(1)**, as follows **[53, 54]**:

$$Removal\ (\%) = \frac{C_i - C_t}{C_i} \times 100, \qquad (1)$$

where C_i is the initial concentration (mg 1^{-1}) and Ct is the concentration of the solution at time *t* (mg 1^{-1}).

Equilibrium adsorption capacity (q_e) and adsorption capacity (q_t) at any instant of time t can also be calculated by the following expressions in equations **(2)** and **(3) [55, 56]**:

$$q_e = v \times \frac{C_i - C_e}{m}, \qquad (2)$$

$$q_t = v \times \frac{C_i - C_t}{m}, \qquad (3)$$

where *m* is the mass of adsorbent in grams and *v* is the volume of solution in liters. It must be noted that q_e is equal to q_t at the last sampling time in the adsorption process.

2.7. Reusability test

For the desorption test, the nanofibers were extracted from the conical flasks containing the hormone solutions and washed thoroughly with distilled water, followed by stirring at a constant 250 rpm for 15 min in deionized water. They were subsequently placed in an oven at 30 °C for 6 h to remove excess moisture and dried in the air; the nanofibers remained unaffected by this. They were then soaked in 40 ml of pure ethanol and continuously stirred for 30 min at 175 rpm to remove the hormones entirely and eluted in ethanol **[1]**. Finally, the nanofibers were dried at room temperature and placed in a desiccator until the next adsorption cycle. The procedure was repeated for several cycles until low adsorption efficiencies were observed.

3. Results and discussion

3.1. Characterization of the electrospun nanofibers

The SEM of the nanofibers, along with the distribution of fiber diameter from the various polymers prepared via electrospinning, are shown in **figure 1.**

The graph above reveals that the uniform nanofibers were produced with minimum beading and a narrow fiber diameter range, i.e 174-330 nm; PU 918 demonstrated the least value and PAN the greatest. These low averages in the size of diameters were attributed to the optimized electrospinning process (low intrinsic viscosity, low polymer concentration in the solution and high electrical conductivity prior to said process); the large surface area was the consequence of this. The size and morphology of the estrogenic hormones were also analyzed on an electron microscope and the micrographs are shown as supplementary data (figure S2).

Applying the average diameter of the nanofibers calculated from SEM, in consideration of the fiber constituting a single continuous cylinder, the length per unit mass (*l/m*) and surface area (A) of the fiber can be calculated by the following equations **(4)-(6) [1]**:

$$V = \frac{m}{\rho} = \frac{\pi d^2 l}{4}. \qquad (4)$$

By rearranging this expression, the following is obtained:

$$l/m = \frac{4}{\rho \pi d^2}, \qquad (5)$$

where V is the volume (m^3), m is the mass (mg), d is the diameter of the nanofiber (m) and ρ is the density of each given polymer (g cm^{-3}).

Since $l >> d$, it is possible to neglect the individual crosssectional area (A) of the end portions of the fibers, such that

total surface area per unit of mass is expressed as:

$$\frac{A}{m} = \frac{d\pi l}{m} = \frac{4}{\rho d}. \qquad (6)$$

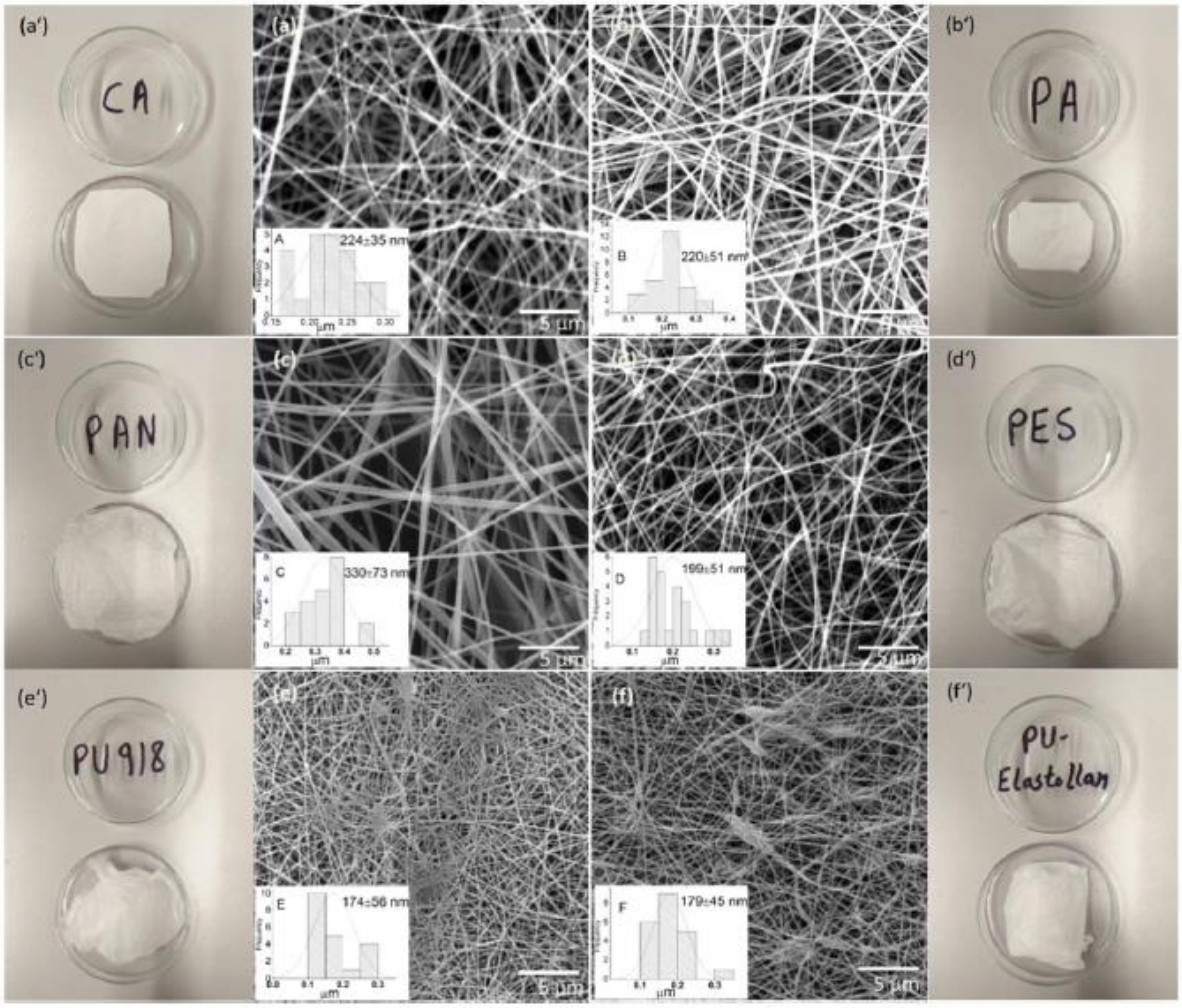

Figure 1. Electron micrographs, (inset) distribution of frequency size and sample images of the electrospun nanofibers (20 mg) of ((a), (a7)) CA, ((b), (b')) PA, ((c), (c')) PAN, ((d), (d')) PES, ((e), (e')) PU 918 and ((f), (f')) PU Elastollan, respectively.

Table 2. Characteristics of the electrospun nanofibers as gauged by BET, contact angle and calculated values from the SEM images.

Nanofiber	Average fiber diameter (nm)	Fiber length per unit of mass (m mg^{-1})	Calculated surface area (m^2 g^{-1})	BET surface area (m^2 g^{-1})	Contact angle(°)
CA	224 ± 35	19 297	13.6	8.66	22.2 ± 0.9
PA	220 ± 51	24 268	16.8	5.50	8.8 ± 2.3
PAN	330 ± 73	9875	10.2	5.16	0
PES	199 ± 51	23 816	14.9	17.66	72.5 ± 1.8
PU 918	174 ± 56	38 231	20.9	5.34	27.4 ± 0.1
PU Elastollan	179 ± 45	32 572	18.3	16.34	45.4 ± 1.1

Table 2 details the recorded diameters from the SEM images, calculated fiber length and surface area through the application of the above formulas, in addition to the surface area measured by BET.

The geometrically determined surface areas, based on SEM, strongly agree with the average fiber diameter because smaller diameter nanofibers possess a larger surface area, which indicates more sites for adsorption. For instance, PU 918 had the smallest average fiber diameter (174 ± 56 nm), so it possessed the largest calculated surface area (20.9 m^2 g^{-1}) and PAN had the largest average fiber diameter (330 ± 73 nm), so it possessed the least calculated surface area (10.2 m^2 g^{-1}); the results correspond to the literature with the values in the range of 9-51 m^2 g^{-1} for surface area and a few hundreds of nanometers for average fiber diameter **[1, 57]**. The estimated surface area of cylindrical geometry was founded on a calculation that assumed the fibers had a smooth surface and no solvent evaporated during electrospinning. Whereas, in BET measurement, the surface area is slightly underestimated because each polymer had a different mass per unit area produced, which could be a plausible reason, especially in PU 918 with 0.7 g m^{-2} (see **table 1**), which has led to a lower value of BET.

The hydrophilic properties of the electrospun nanofibers were tested using contact angle measurements. It is considered that the hydrophilic surfaces generally have a contact angle of <90° and the lesser the contact angle, the more hydrophilic the material is. We observed that the liquid instantly penetrated the nanofibers on pp completely. Therefore, nanofibers were compressed on a PET sheet and it exhibited low contact angle values because we observed water percolation into fiber networks. According to the results obtained **(table 2)**, the contact angle values were in the range of 0°-72.5°. These values indicated that all the nanofibers were hydrophilic and suitable for the removal of the investigated estrogenic hormones. The contact angle of a particular polymer's nanofibers mainly depends on the concentration of the polymer in solution during the electrospinning process. The possible reasons for the difference in contact angles of various polymer nanofibers could be their structure, pore size and fiber diameter **[58]**.

IR studies were conducted to distinguish the functional groups in the electrospun nanofibers of each polymer which are later discussed in the adsorption mechanism section to understand the type of bonding and interactions between estrogenic hormones and nanofibers, as shown in **figure 2**.

As can be seen from **figure 2**, the characteristic peaks for PAN at 1250, 1454, 1667, 2243 and 2927 cm^{-1} correspond to C-N stretching, C-H bending in CH_2, C=C stretching, C=N stretching and C-H stretching vibrations in the polymer structure, respectively **[59]**. The small PAN and polyurethanes peaks represent aliphatic CH_2, reflecting a C-H asymmetrical flexing vibration. The electrospun polyurethanes show an absorption peak at 3330 cm^{-1} caused by the stretching vibrations of N-H and the aliphatic amino group in the carbamate. Strong peaks usually occur between 1700 and 1736 cm^{-1}, relating to mono or disubstituted compounds, herein denoting the peak at 1732 cm^{-1} attributed to the C=O stretching vibration of the amido ester, while a separate region at 1701 cm^{-1} is observed for PU Elastollan in contrast with a single peak at 1715 cm^{-1} for PU 918. The peak at 1529 cm^{-1} is for N-H bending and C-N stretching vibrations of the amide group. The peak at 1224 cm^{-1} arises through the C-N stretching vibration for the other amide group. As a result of the stretching vibration of the C=C bond in the skeleton of the benzene ring, peaks appear at 1476 and 1597 cm^{-1}. A broad range of peaks occurs at 1079 and 1106 cm^{-1} due to characteristic bands of alkyl ether causing the asymmetric flexing vibration of C-O-C bonds, most prominent for PU Elastollan **[60, 61]**.

The vibration of aromatic hydrocarbons is observed in PES at the bands 1577, 1485 and 1105 cm^{-1}. The bands at 1241 and 1150 cm^{-1} could be due to aryloxide and aromatic sulfone groups, respectively. A

band arising through a SO_3H symmetrical stretching vibration appears at 1011 cm^{-1}. These peaks indicate that the material is strongly sulfonated **[62]**.

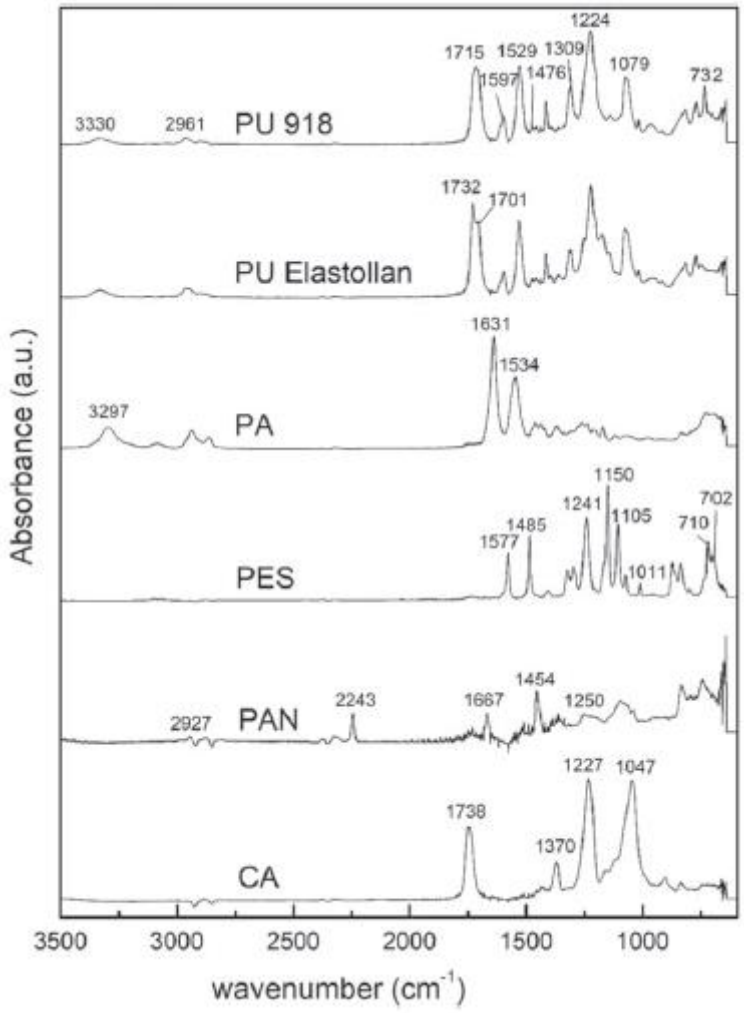

Figure 2. FTIR spectra for the electrospun nanofibers from attenuated total reflectance (ATR) sampling.

The peaks at 710 and 702 cm^{-1} are attributed to the stretching vibrations of C-O and C-S bonds, respectively **[63]**.

The peak at 1534 cm^{-1}—characteristic of PA—is attributed to amide II, C=O bending and the amide I band at 1631 cm^{-1} indicates the stretching vibration of C=O in the amide group (-CO-HN-). Lastly, the amide A band at 3297 cm^{-1} corresponds to -NH stretching **[64]**. In the case of CA, it can be seen that the vibration peak at 1047 cm^{-1} shows a C-O bond, the peak at 1227 cm^{-1} represents a (C-O-C) antisymmetric stretching ester group, the peak at 1370 cm^{-1} denotes C-CH3 and the peak at 1738 is for C=O bond stretching of the carbonyl group **[65, 66]**. Hence, the FTIR spectra measured for the nanofibers are in reasonable compliance with spectra for the original polymeric raw materials from the bank of IR spectra.

3.2. Static adsorption study of hormones on the polymeric materials

The experiment was conducted on 100 ml of a solution containing a mixture of the 4 estrogenic hormones (E1, E2, EE2, E3) at a total concentration of 0.8 mg 1^{-1}, wherein each hormone equated to 0.2 mg 1^{-1} in concentration, in addition to 20 mg of adsorbent. **Figure 3** details the static adsorption of each hormone separately on the various electrospun nanofibers at 250 rpm over a period of 9 h.

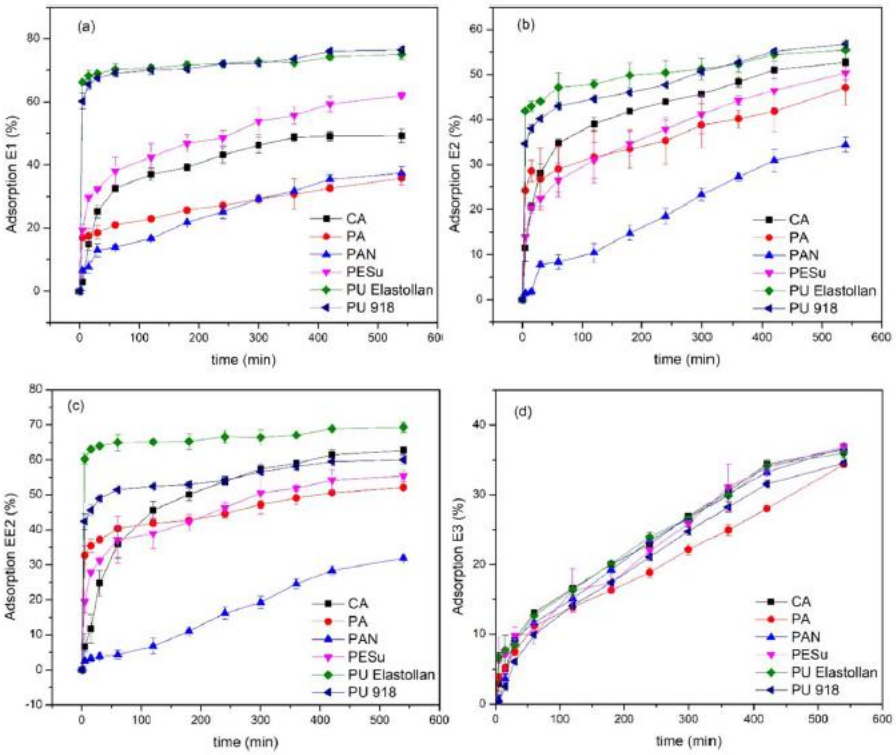

Figure 3. Static adsorption of each estrogenic hormone on six different nanofibers from a combined solution of (a) E1, (b) E2, (c) EE2 and (d) E3.

The results in **figure 3** demonstrate that polyurethanes were most efficient at removing EE2, E2 and E1, PAN demonstrated the lowest capacity for EE2 and E2 adsorption, while PA was the least effective with E1 and E3. The plausible reason for the least adsorption on PAN could be due to its large fiber diameter (330 ± 73 nm), as depicted by its least calculated total surface area of 10.2 m^2 g^{-1} compared to the other polymers, thereby attributing to its less available sites for adsorption and hydrogen bond interactions with the estrogenic hormones. Comparing the sorption efficiency of both polyurethanes revealed that PU Elastollan either possessed a superior adsorption effect (for the hormones EE2 and E2) or was identical (E3, E1), potentially due to the lesser content of hard segments in PU Elastollan than PU 918. The active sorption center of PU Elastollan is more easily accessible than the sterically hindered center in the hard segments of PU 918.

All materials showed a similar trend of sorption for the E3 hormone. The conclusion can be drawn that EE2, E2 and E1 were readily adsorbed by these nanostructured materials, with E3 being adsorbed the least. The low percentage of removal of E3 could be attributed to its minimal log K_{ow} value of 2.45, compared with E1, E2 and EE2 at 3.43, 3.94 and 4.15, respectively. The adsorption of these estrogens was directly related to their hydrophobic nature, as specified by the higher value for K_{ow} **[54]**.

Furthermore, E3 followed a different kinetic trend than the other hormones in that its adsorption was gradual, whereas most of the adsorption of the other hormones occurred within the first 70 min for the majority of the materials. CA and PES had similar adsorption behavior for all the hormones and CA exhibited higher adsorption efficiency for EE2 and E2, though PES was particularly effective with E1. Therefore, it is noteworthy to mention that every material proved sufficient in its response to simultaneous adsorption of each hormone.

3.3. Equilibrium adsorption capacity comparison

Determination was made as to total adsorption in combination for all four hormones by each polymer, along with cumulative adsorption capacity as a function of time to work out the overall efficiency of each polymer. The various trends are presented in **figure 4**.

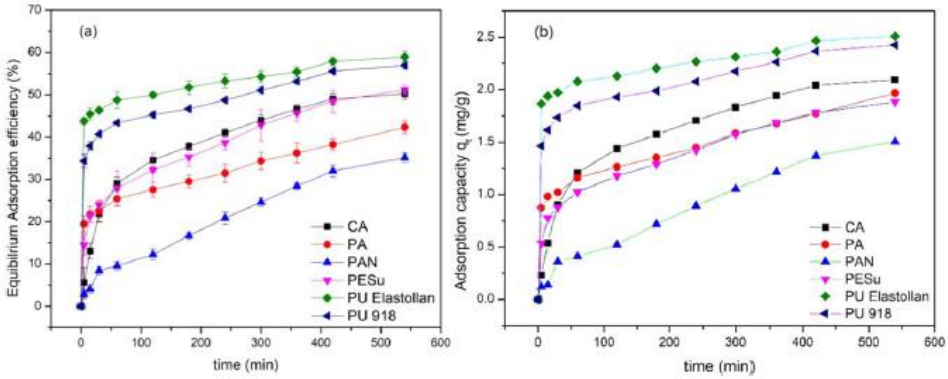

Figure 4. Trends for the combined hormones of E1, E2, EE2 and E3 on the nanofibers as to (a) removal efficiency as a function of time and (b) total adsorption capacity as a function of time.

Figure 4(a) above shows the total cumulative adsorption of the hormones on the nanofibrous materials to the time of 540 min for equilibrium. The results show that the removal efficiency at equilibrium for the different materials ranged between 30% and 60%. The graph reveals that the polyurethanes had the greatest tendency and fastest rates for adsorption, reaching close to equilibrium with 50% efficiency within the first 100 min, as represented by the initial curve of the graph, reaching a maximum removal efficiency of ca. 60%. Although PAN initially had the lowest rate, it eventually demonstrated the highest rate at the halfway point between 120 and 420 min, as visible in the steepness of the curve. CA and PES were similar in adsorption behavior, reaching 50% at equilibrium. Thus, PU Elastollan was the best polymer for adsorption of the estrogens, with PAN being the least effective.

The total adsorption capacity of each material as a function of time is detailed in **figure 4(b)**. The results indicate that the cumulative adsorption capacity of the four estrogenic hormones increased for each material until equilibrium was established between the adsorbates and adsorbent. The time to reach equilibrium depended on the concentration of the adsorbate and the amount of adsorbent **[67]**. Both factors were kept constant to compare the capacities of the different materials. However, it was still necessary to increase the amount of adsorbent to enhance the removal efficiency of the polymers over a shorter time frame. The highest cumulative adsorption capacity calculated was 2.51 mg g^{-1} for PU Elastollan, whereas the lowest was 1.51 mg g^{-1} for PAN. The adsorption capacities for E1, E2, EE2 and E3 were found to be 0.801, 0.592, 0.736 and 0.382 mg g^{-1} for PU Elastollan and 0.396, 0.370, 0.343 and

0.397 mg g^{-1} for PAN, respectively. EE2 stood out in terms of adsorption and was found to have the highest adsorption capacity for all the polymers compared to the other estrogens.

Thus, the results of polymers in the current study are well in compliance with the literature values and comparing the adsorption capacities herein with previous research showed the suitability of these polymers as a potential adsorbent for removing the estrogenic hormones, in comparison with solid particles and membranes. Adsorption capacities reported in the literature were found to be 0.423 mg g-1, 0.472 mg g^{-1} and 0.472 mg g^{-1} when MWCNTs was used and 2533.34 ng g^{-1}, 2020.78 ng g^{-1} and 2234.09 ng g^{-1} when activated sludge was employed for E1, E2 and EE2, respectively. The value for removing E1 was 62 ng g^{-1} via a hydrophobic hollow fiber membrane **[54]**. Hence, PU Elastollan in the current study has a higher adsorption capacity for each hormone compared to the research in the literature. Another aspect that distinguishes these polymeric membranes over solid particles is that solid particles require a further sophisticated purification method to be separated from the treated water, which increases the cost. In addition, solid particles sometimes are toxic, which makes them less preferable for the intended purpose. Whereas these nanofibers can be easily washed, reused and the estrogenic hormones can be quickly recovered. Furthermore, environment-friendly nanoparticles as adsorbents can be used as additives in these nanofibers during electrospinning which can further enhance their adsorption capacity by increasing the surface area and available sites that can be viable for the entrapment of estrogenic hormones.

3.4. Adsorption kinetics

Removal of the estrogenic hormones by the polymer nanofibers through adsorption increased over time, obtaining a maximum value for every hormone on each polymer type and reaching equilibrium. The adsorption rate was initially rapid until 30 min had passed, whereupon it gradually ebbed away in parallel with the duration of contact, to an assumed plateau at 540 min.

The results obtained from the experiment were employed to investigate factors affecting the adsorption process and the rate-limiting step in the process, such as the transfer of mass and type of chemical interaction. Furthermore, the kinetics for selecting optimum conditions for full-scale removal of the hormones were studied. It is often difficult to determine kinetic parameters and explain the mechanisms involved in complex heterogeneous systems since surface effects can be superimposed on top of chemical effects. Therefore, to further understand such adsorption behavior and mechanisms, parameters from three models—pseudo-first-order, pseudo-second-order and Weber-Morris intraparticle/membrane diffusion model equations—were employed to test the experimental data and examine the adsorption kinetics of the four estrogenic hormones taken up by each polymer. These models are applicable for describing liquid/solid systems. Pseudo-first-order constitutes a widespread, commonly applied model for analyzing the adsorption of a solute in an aqueous solution. In this context, the rate of sorption of hormones on the surface of the nanofibers was proportional to the amount of hormones adsorbed from the solution phase, expressed by equation **(7)** as **[68]**:

$$q_t = q_e(1 - \exp(-k_1 t)), \qquad (7)$$

where q_t is the amount of hormone adsorbed per unit mass at time t (mg g^{-1}), q_e is the amount of hormone per unit mass at equilibrium (mg g^{-1}) and k_1 is the first-order rate constant (1 min^{-1}).

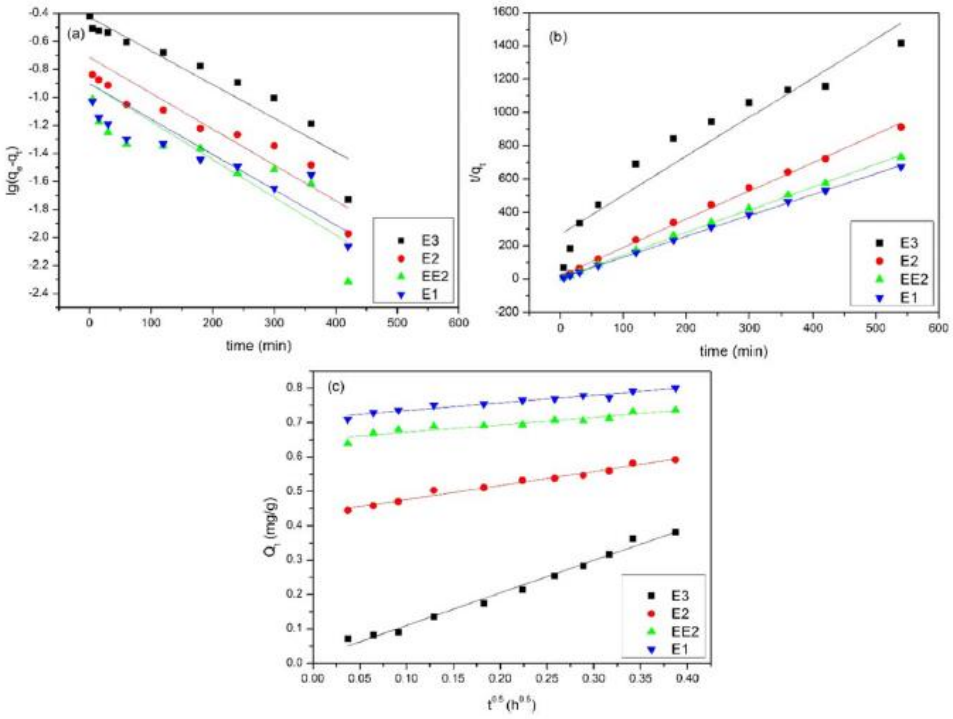

Figure 5. Plots of the adsorption kinetics for the four estrogenic hormones (E1, E2, EE2, E3) on PU Elastollan nanofibers: (a) pseudo-first-order, (b) pseudo-second-order, (c) the Weber-Morris interparticle diffusion model.

The pseudo-second-order equation relates to solid-phase adsorption capacity and can predict the behavior of kinetics over a great range for adsorption **[69]**. In this model, surface adsorption is the rate-determining step, which involves chemisorption due to physicochemical interactions between the solid and liquid phases **[70]**. The linear form of equation **(8)** is expressed as **[71]**:

$$\frac{t}{q_t} = \frac{1}{k_2 q_e{}^2} + \frac{t}{qe}, \qquad (8)$$

where k_2 is the reaction rate constant (g (mg min)$^{-1}$).

The adsorption process usually occurs in consecutive steps, comprising movement of the adsorbate from the solution bulk to the surface of the adsorbent and then diffusion through the boundary layer to the outer surface of the adsorbent. This is followed by adsorption on an available active site on the surface of the adsorbent and, finally, intraparticle diffusion through pores. The Weber-Morris intra-particle/membrane diffusion model is diffusion-controlled; the adsorption rate directly depends on the speed at which an adsorbate can diffuse towards the adsorbate. This model is described by equation **(9)**, as follows **[72]**:

$$q_t = kt^{\left(\frac{1}{2}\right)} + I, \qquad (9)$$

where k is the reaction rate constant (mg g^{-1} $h^{1/2}$) and I is the y-intercept constant (mg g^{-1}) providing data on the thickness of the boundary layer.

For the validity of this model, it is essential to note that the linear, converging line for each estrogenic hormone must pass through the point of origin for intraparticle diffusion to constitute the rate-determining step.

Figure 5 contains plots describing the adsorption kinetics of the four estrogenic hormones on PU Elastollan since this polymer exhibited the highest removal efficiency, adsorption capacity and has proven to be the best nanofiber; the kinetic parameters obtained are given in **table 3**. The kinetic plots and parameters for the other polymers were also calculated and are provided in the supplementary data (figures S3-7 and tables S1—5).

Table 3. Values for each hormone from the kinetic models in relation to PU Elastollan electrospun nanofibers.

	Experimental	Pseudo-first-order model			Pseudo-second-order model			Intraparticle diffusion model		
Hormone	q_e (mg g^{-1})	k_1 (min^{-1})	q_e, cal (mg g^{-1})	R^2	k_2 (g mg^{-1} min^{-1})	q_e, cal (mg g^{-1})	R^2	k (mg g^{-1} $h^{1/2}$)	I (mg g^{-1})	R^2
E3	0.382	0.002	0.373	0.901	0.020	0.426	0.924	0.947	0.015	0.987
E2	0.592	0.003	0.193	0.793	0.145	0.589	0.998	0.406	0.436	0.983
EE2	0.736	0.003	0.125	0.630	0.276	0.733	0.999	0.219	0.650	0.895
E1	0.801	0.003	0.125	0.619	0.286	0.796	0.999	0.228	0.711	0.946

The results were examined to obtain fits for the adsorption kinetics of the adsorbate mixture of E1, E2, EE2 and E3 estrogenic hormones on the adsorbent nanofibers by plotting on graphs the pseudo-first-order, pseudo-second-order and Weber and Morris intraparticle diffusion models. **Figure 5(a)** shows $lg(q_e\text{-}q_t)$ plotted against t for the E3 hormone, which is in good compliance with the pseudo-first-order equation. The data points are shown together with generated lines for best fits. The agreement between the data set is reflected in the high regression coefficient (0.901) for E3 compared to the other three hormones (E2, EE2 and E1) with the regression coefficients 0.793, 0.630 and 0.619, respectively. The equilibrium adsorption capacity calculated for E3 (0.373) is reasonable compared to the experimental value (0.382). The rate constant k_1 is far more similar, though and within the range for all hormones. For E2, EE2 and E1, however, this model appears to be less accurate for describing the initial stage ($t \leq 30$ min) and the theoretical expected yield of 0.193, 0.125 and 0.125 seems unsatisfactory and much lower than the actual values of 0.592, 0.736 and 0.801 for E2, EE2 and E1, respectively.

The lines plotted in **figure 5**(b) of t/q_t versus t have to be linear to estimate q_e and k_2 from the curve and y-intercept, respectively. The results indicate that the interaction of E2, EE2 and E1 with the material followed second-order kinetics, as shown by the line for best fit adhering fully with the data set points. The regression coefficients are greater than 0.99 and the calculated adsorption capacities of 0.589, 0.733 and 0.796 are incredibly close to the experimental values 0.592, 0.736 and 0.801, respectively. This suggests that the active sites were not homogeneous on the surface since the rate of adsorption is determined by two factors—the concentration of the hormones and the number of active sites available on the material **[67]**. These findings confirm the suitability of this model for describing the adsorption of E2, EE2 and E1 on the PU Elastollan nanofibers. Similar results were observed for the other polymers in this study compared with results described in the literature for MWCNTs **[54]**. E3 exhibits an overall mismatch, though, as two linear portions are visible— one for the first 60 min and another for the period after 100 min. The plot in **figure 5(b)** was applied to determine

the rate constant (k_2) and the calculated equilibrium adsorption capacity (q_e) expressed in equation (8) to obtain the regression coefficient (R_2) shown below in **table 3**.

In the case of q_t versus $t^{0,5}$, the graph for E3 is linear in progression with a comparatively high and acceptable regression coefficient (0.987) that almost passes through the point of origin. This means that intraparticle diffusion constitutes the rate-limiting step, which is unlikely to happen in the adsorption of the other three hormones (see **figure 5**(c)). The plots for the other estrogens do not pass through the point of origin, potentially due to a surface effect that may have controlled the sorption process during the initial time periods, representing a diffusion-controlled or boundary layer diffusion effect. Thus, for E2, EE2 and E1, intraparticle diffusion could comprise part of the mechanism, though not a step for determining the total rate of diffusion. The values calculated by equations **(7)-(9)** are given in **table 3**.

3.5. Adsorption mechanism

The possible mechanisms that existed between the estrogens and nanofibers comprise the following: (1) size-exclusion; (2) physical adsorption of estrogens on the external surfaces and inside layers of the nanofibers due to their porous structures; (3) charge interactions between the estrogens and electrospun nanofibers; (4) the bonding of estrogen molecules onto the nanofibers via reaction with the functional groups present on the surfaces of the nanofibers. Size exclusion would not be expected in this system as the reported molecular size of the estrogens was quite small (approximately 0.8 nm for E1 and 0.796 nm for E2), compared to the pore sizes of the electrospun nanofibers and GMF filter used; otherwise, their removal efficiency would have been 100%.

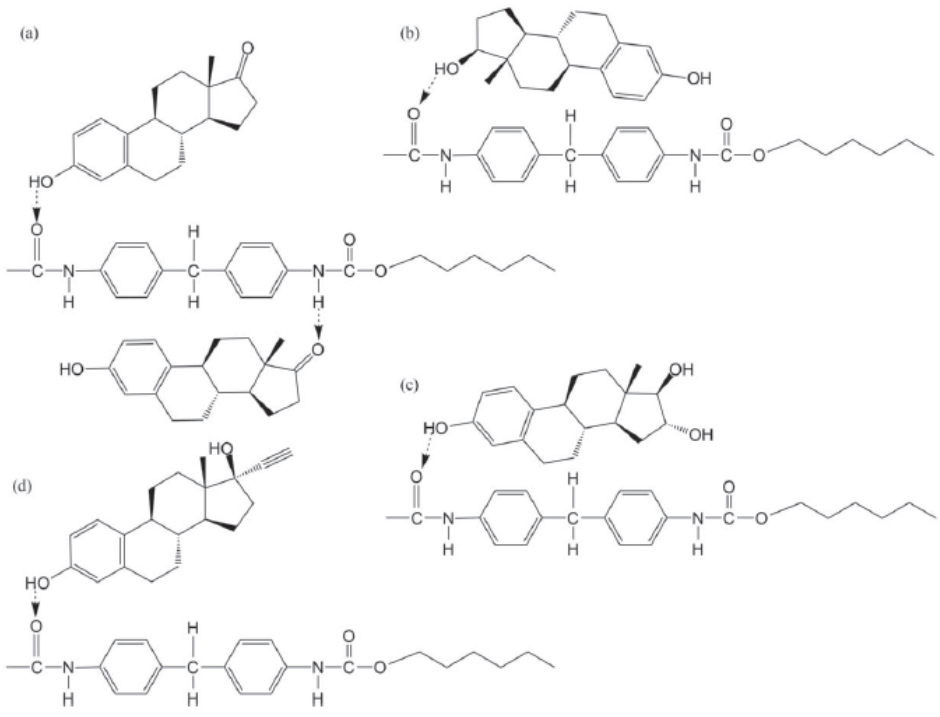

Figure 6. Hydrogen bonding between the polyurethane molecule and estrogenic hormones (a) E1, (b) E2, (c) E3 and (d) EE2.

As the fiber diameters of the polyurethanes were lesser in size (PU 918 = 174 ± 56, PU Elastollan = 179 ± 45), their surface area is larger as a consequence (20.9 and 18.3, respectively), providing sufficient availability of active sites for adsorption of the estrogens, as detailed in **table 2**. Electrostatic charge can also affect adsorption, as Porter and Porter report in the literature on adsorption behavior on microfilters in the presence of cations **[73]**. The deprotonation of E1, E2, EE2 and E3 is governed by the dissociation of the hydroxyl group attached to the benzene ring. The acid dissociation constants for E1, E2, EE2 and E3 equal 10.34, 10.46, 10.4 and 10.38, respectively **[74, 75]**. All of them have slightly weaker acidity than phenol (pK_a = 10). As a result of the high value of *pKa*, most of the molecules of the estrogens were undissociated and thus, they remained neutral in the solution mixture **[9]**. Therefore, it is unlikely that charge interaction was the main factor that brought about the significant adsorption of the estrogenic hormones on the nanofibers **[8, 76]**.

The high and rapid adsorption of the estrogens on the polyurethanes is noteworthy. The molecules were far smaller in size than the porosity of the nanostructures, indicating that pore size had a negligible dependence on adsorption. Apart from physical adsorption, which gradually reaches equilibrium, the only rational explanation for the strong interaction of these estrogens with the nanofibers is bonding. Hydrogen bonds are stronger than Van der Waals forces involved in physical adsorption. In this context, **figure 6** presents the chemical interactions of each estrogen with the polyurethane molecule.

Each estrogen molecule (E1, E2, EE2, E3) in this study contains a hydroxyl group (-OH) acting as a proton donor for hydrogen bonding. Due to the presence of both a nucleophilic carbonyl group (-C=O) and hydroxyl group in E1, this proton can act as both a donor or acceptor in hydrogen bonding and has the highest removal efficiency as a consequence. Han *et al* describe similar hydrogen bonding by E1 with nylon 6,6 membrane in their research **[8, 64]**. Nylon 6,6 and polyurethanes possess identical functional groups involved in hydrogen bonding. Therefore, the functional groups (N-H and C=O) in PU Elastollan, PU 918 and PA participated in the hydrogen bonding of E1, although only C=O was present for the other three estrogens, as determined by FTIR analysis.

These hydrogen bonding interactions would dictate the adsorption of the estrogens on the polyurethane nanofibers, explaining the rapidity of the adsorption process in the initial stage of the experiment. The accurate technique of FTIR analysis was employed to characterize hydrogen bonds on the PU 918 polyurethane, as detailed below.

The FTIR spectra for a PU 918 sample saturated with estrogen are presented in **figure 7**. A notable aspect is the difference in the relative intensity of the peak at 1715 cm^{-1} that corresponds to C=O stretching. A crucial feature of PU 918 is its cross-linking molecular structure that arises through inter and intra-hydrogen bonds. The band contributes to restricting the stretching of the hydrogen bonds on the carbonyl group in PU 918 and is evident from the shift of the peak to a reduced frequency of 1700 cm^{-1}. There is also a significant drop in intensity at 1715 cm^{-1}, yet this is not the case for two amide bands (at 3330 cm^{-1} and 1529 cm^{-1}), suggesting a change occurs through adsorption of the estrogenic hormones. A possible explanation could be the presence of hydroxyl groups on the terminals of the estrogens that compete with -NH groups in acquiring the carbonyl groups present on the polyurethane; this potentially causes weak intermolecular hydrogen bonding, with eventual substitution by the estrogen molecules and the subsequent formation of new bonds.

No notable change occurs for the amide band (3330 cm^{-1}) after adsorption. A possible explanation is that the -NH groups are not set free to interact with hydrogen donors, such as the water and C=O groups of the cyclopentane rings present in E1 molecules, so it cannot forge new hydrogen bonds; otherwise, a new peak would be visible at ca. 3400 cm^{-1} **[64]**. Han et al report that N-methyl acetamide

(NMA), which possesses a simple structure with an amide group, does not interact with the -C=O group when released. The results are given herein clearly agree with the study in the literature; thus, the estrogens (E1, E2, EE2, E3) under investigation might form hydrogen bonds with the polyurethanes and PA **[76, 77]**.

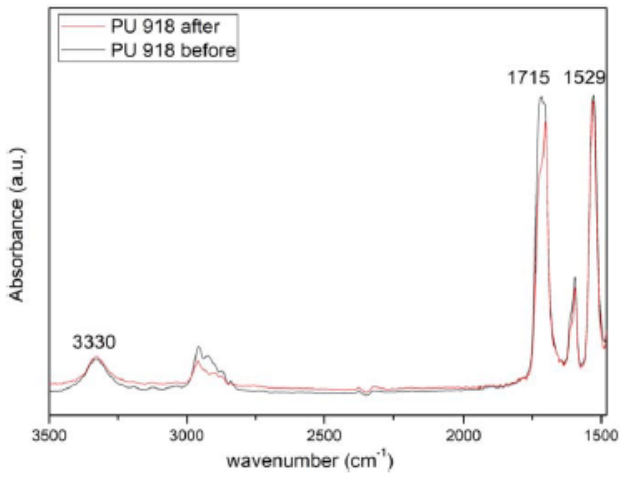

Figure 7. FTIR spectra for the PU 918 nanofibers before and after static adsorption (0.8 mg 1^{-1} mixture of E1, E2, EE2 and E3 of 100 ml volume)

3.6. Determination of recovery and reusability

In order to determine the reversibility of the polymers for sorption, triplicates of each polymer sample were soaked in 50 ml of water and shaken for 15 min, which would not significantly reduce the hormone concentration on the nanofibers as a consequence of chemical bonding **[1]**. Therefore, each sample, after being washed three times with distilled and deionized water, was immersed in 40 ml of pure anhydrous ethanol since all estrogenic hormones exhibit very high solubility in ethanol due to their high partitioning coefficient (Log- $K_{o/w}$ = 3.13, 4.01, 2.45 and 3.90 for E1, E2, E3 and EE2, respectively). A strong partitioning effect was expected to occur in combination with a competing hydroxyl group present in the ethanol, which could destabilize the estrogen-nanofiber hydrogen bonds and attract the adsorbed hydrophobic hormones in the ethanol solution **[8, 64]**. The resultant solution was gently stirred for 30 min at 175 rpm and air-dried afterward, a process repeated up to four consecutive cycles. **Figure 8** presents the adsorption study over the four cycles.

The above graphs represent the removal of the hormones in percentage, present at 0.2 mg 1^{-1} in concentration with 20 mg of each nanofiber adsorbent over four adsorption cycles. As can be seen, the trend is one of decrease for each material after consecutive cycles for all the hormones, except for PES during the second and third cycles as it underwent the least change in surface morphology; the change in average fiber diameter from the original size of 199-278 nm following ethanol treatment was not as large as for other polymeric nanofibers. The highest removal efficiency is evident for E1 and EE2, with the least for E3. The values for removal efficiency are similar for all the materials during the first cycle of E3. PA shows the least adsorption for E1 and E3, while PAN exhibits the least for EE2 and E2. Notably, PAN cannot be reused for E1 because of the significant effect that transpires during the desorption process, leading to a loss in mass, which brings about a decrease in the amount of active adsorption sites and reduction in the surface area through an increase in fiber diameter.

PU 918 appears applicable for removing E1 and E2 during the first cycle, whereas PES and PU Elastollan are more suited to E3 and EE2, respectively. A drastic drop in the effectiveness of the materials for E1 and E3 arises during the second cycle, possibly related to the treatment with ethanol they received in the desorption process. However, this is unlikely to occur in the case of EE2 and E2, as the materials seem far more reliable over repeated cycles. It can be concluded that the adsorbent materials under investigation are reusable to a limited extent after being washing with ethanol, i.e up to four adsorption cycles, with the exception of E3 with a limit of three cycles.

The comparison presented was conducted to discern the reusability of the nanostructured sorption materials. Industrial applications may require the testing of other solvents and the findings reported herein indicate that the suitable solvent must possess very high solubility of hormones but minimum solubility of these polymers from which the nanofibers were made. **Figure 9** shows the overall efficiency of each polymer over four adsorption cycles.

Figure 9 illustrates the adsorption efficiency of each polymer for cumulative estrogenic hormone removal over four adsorption cycles. It should also be noted that these percentages are for the mixture of E1, E2, EE2 and E3 for each polymer per cycle. PU Elastollan demonstrates the highest extent of hormone removal in the first cycle, in contrast with PAN with the least, while PU 918 has the highest efficiency in the 4th cycle. PA exhibits the least drop in effectiveness from the first to the second cycle and better reliability. PES is the most consistent and manages the greatest adsorption in the 3rd cycle. It should be noted that due to repeated treatment with ethanol during desorption, it was evident that the nanofibers became stiff and shrank due to loss in mass until the last cycle. Compact and tightly folded, they provided less surface area for hormone entrapment during the final cycle, as shown in **figure 10**.

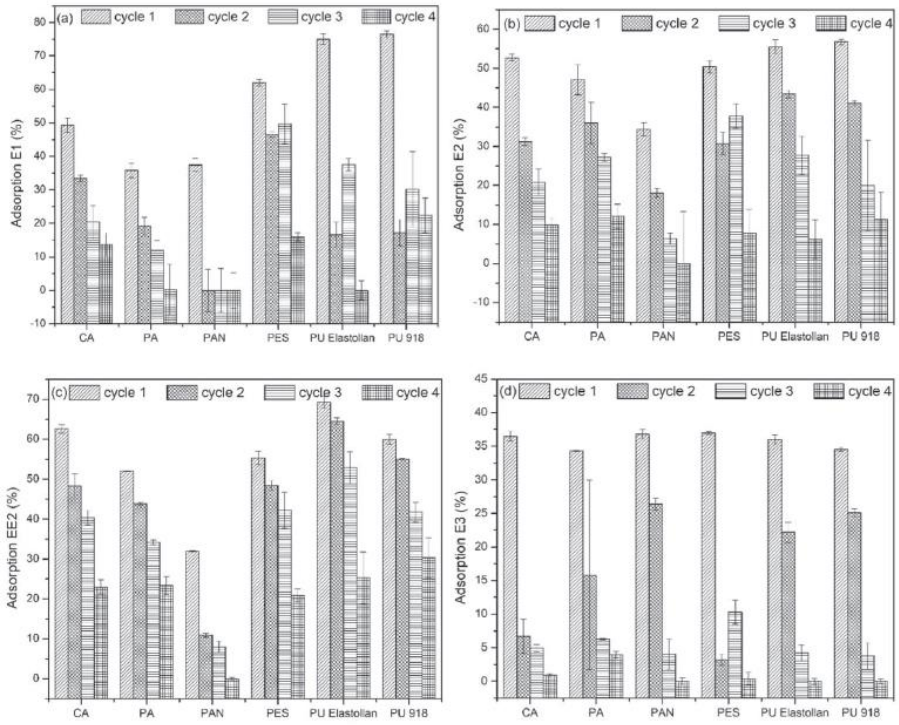

Figure 8. Four adsorption cycles for each electrospun material (20 mg) and each estrogenic hormone (a) E1, (b) E2, (c) EE2 and (d) E3, at an initial concentration of 0.2 mg 1^{-1} in a combined solution of 0.8 mg 1^{-1}.

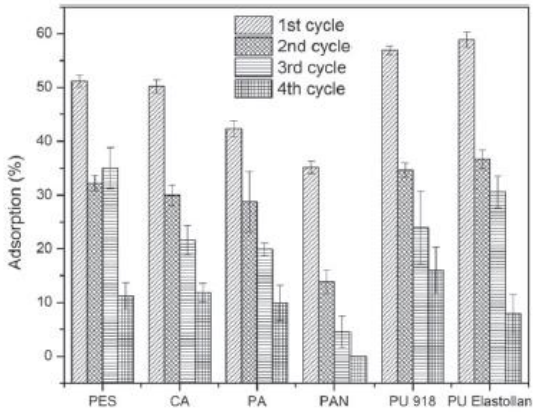

Figure 9. Cumulative efficiency of adsorption for the four estrogenic hormones on the various nanofibers over four cycles.

The repeated desorption cycles of estrogen hormones from the nanofibers, wherein ethanol was applied, exerted a significant change in fiber morphology attributed to contact between the nanofibers and ethanol. The nanofibers of these materials are not prone to dissolving in ethanol and their porous structure facilitates the complete penetration of ethanol molecules. This is why, after several cycles and a period of contact, the structure of the nanofibers collapsed and swelled and the effectiveness of the adsorption process diminished, as is evident in the SEM images of the nanofiber structures after four cycles in **figure 10**.

Figure 10 presents the surface morphology for each nanofiber after four adsorption-desorption cycles. It is visible that the diameter of the nanofibers increased for each type of polymer, ranging from 249 to 475 nm (PU Elastollan experienced the least and PAN the highest), in comparison with the range in diameter prior to adsorption, which was 174-330 nm, respectively.

3.7. Limitations, future works and practical application

This is a preliminary model study for testing various electrospun polymers for simultaneous adsorption of a set of four estrogenic hormones using ultrapure water. However, certain limitations exist that require extra investigation and improvement to devise a continuous adsorption technique that functions at high pressures. Additionally, several aspects of the process that include membrane fouling, solution characteristics, varying concentrations of adsorbent and adsorbate need to be addressed to make this process amenable for large scale use. Future works shall encompass testing the electrospun materials with actual water samples from a reservoir. Doing this would enable the authors to observe the competing behavior and influence of inorganic ions and organic pollutants on entrapping estrogens during continuous adsorption by dead-end flow and cross-flow measurements. A similar concept for research could involve varying the pH, temperature, ionic strength and concentration of adsorbent and adsorbate in order to discern the optimum applicability of kinetics and determine thermodynamic parameters. These matters will be subjected to in future research.

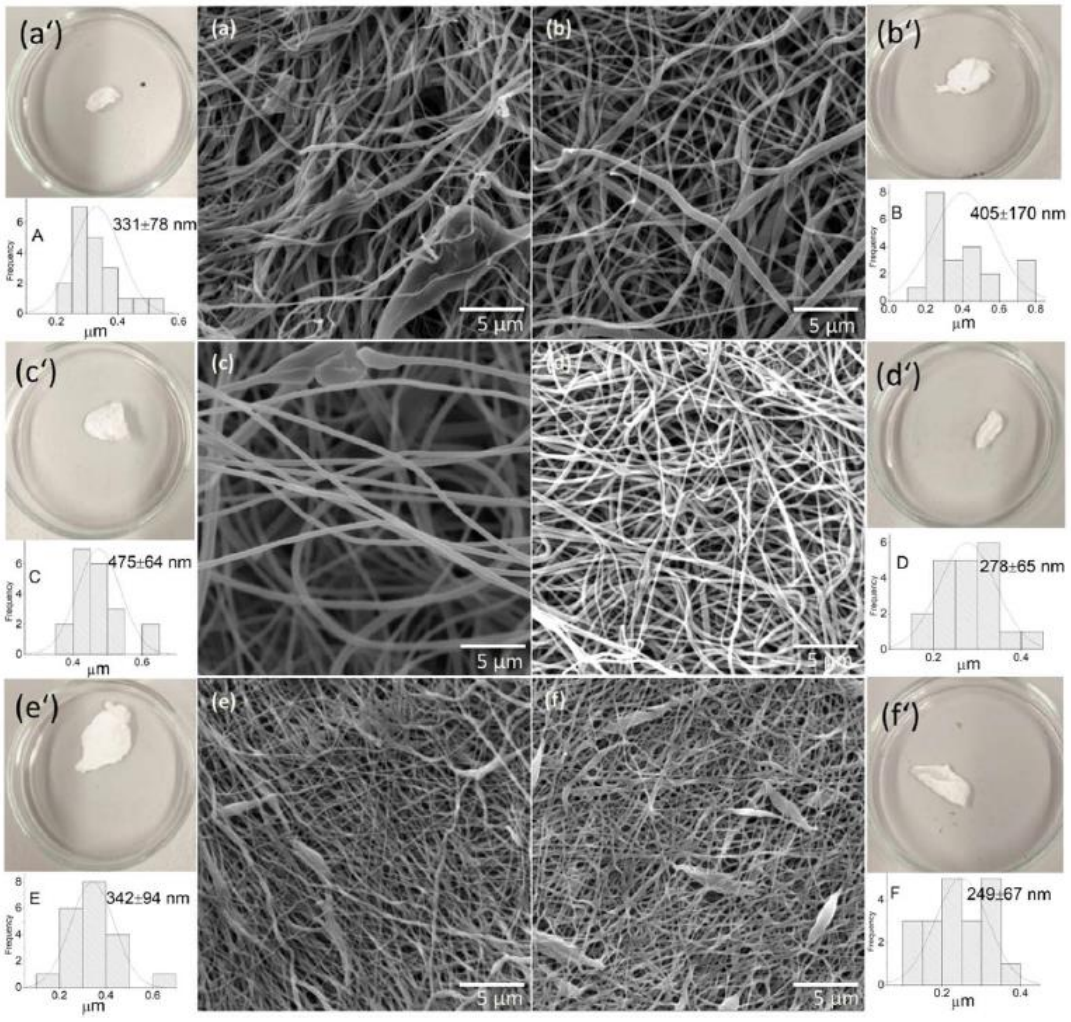

Figure 10. SEM Images, sample images of the nanofibers and distribution of their fiber diameter after four adsorption-desorpton cycles: ((a), (a'), (A)) CA, ((b), (b'), (B)) PA, ((c), (c'), (C)) PAN, ((d), (d'), (D)) PES, ((e), (e'), (E)) PU 918 and ((f), (f'), (F)) PU Elastollan.

4. Conclusions

This study investigated the simultaneous removal of various estrogenic hormones by polymeric electrospun nanostructures. A one-step group detection method was devised for concurrent quantification of the estrogenic hormones. It was found that all the nanofibrous membranes were capable of successfully removing all types of estrogens. Overall adsorption efficiency diminished in the following order: PU Elastollan >PU- 918 >PES >CA >PA >PAN. The chemical composition and functional groups in the structure of the nanofibers played a major role in possessing hydrogen bonds between different types of estrogens and nanofibers, elaborated in the adsorption mechanism. The percentage efficiency of removal was the greatest for E1 (76.5), declining through EE2 (69.3) and E2 (56.8) to E3 (37.0). PU Elastollan demonstrated the highest capacity for total adsorption over the other NF membranes and also compared to literature values, equaling 2.51 mg g^{-1} due to its carbonyl functionality and surface area. Based on results from kinetic models for all the polymers, pseudo-first-order is applicable for E3, with pseudo-second-order being suitable for E1, E2 and EE2; the exception is PAN, where the estrogens follow the pseudofirst-order kinetic model. Consequently, both models are considered appropriate due to their high regression coefficients compared to other kinetic models.

Desorption tests to discern recovery of the hormones and the reusability of the sorption nanostructures were conducted and found to be valid for four cycles. The research carried out shows that polymeric nanofibrous membranes are worthy of consideration as potential adsorbents for the simultaneous removal of estrogens from wastewater streams.

References

[1] Schäfer A I, Stelzl K, Faghih M, Sen Gupta S, Krishnadas K R, Heiβler S and Pradeep T 2018 Poly(ether sulfone) nanofibers impregnated with β-cyclodextrin for increased micropollutant removal from water ACS Sustain. Chem. Eng. 6 2942-53

[2] McLachlan J A, Simpson E and Martin M 2006 Endocrine disrupters and female reproductive health Best Pract. Res. Clin. Endocrinol. Metab. 20 63-75

[3] Montes-Grajales D and Olivero-Verbel J 2015 EDCs databank: 3D-structure database of endocrine disrupting chemicals Toxicology. 327 87-94

[4] Gyllenhammar I, Glynn A, Jonsson BAG, Lindh C H, Darnerud P O, Svensson K and Lignell S 2017 Diverging temporal trends of human exposure to bisphenols and plastizisers, such as phthalates, caused by substitution of legacy EDCs? Environ. Res. 153 48-54

[5] Sood S, Shekhar S and Santosh W 2017 Dimorphic placental stress: a repercussion of interaction between endocrine disrupting chemicals (EDCs) and fetal sex Med. Hypotheses 99 73-5

[6] Luo L, Yang Y, Xiao M, Bian L, Yuan B, Liu Y, Jiang F and Pan X 2015 A novel biotemplated synthesis of TiO2/wood charcoal composites for synergistic removal of bisphenol A by adsorption and photocatalytic degradation Chem. Eng. J. 262 1275-83

[7] Chen Y, Zhang Y, Luo L, Shi Y, Wang S, Li L, Long Y and Jiang F 2018 A novel templated synthesis of C/N-doped /3-Bi2O3 nanosheets for synergistic rapid removal of 17a-ethynylestradiol by adsorption and photocatalytic degradation Ceram. Int. 44 2178-85

[8] Han J, Qiu W and Gao W 2010 Adsorption of estrone in microfiltration membrane filters Chem. Eng. J. 165 819-26

[9] Nghiem L D and Schafer A I 2002 Adsorption and transport of trace contaminant estrone in NF/RO membranes Environ. Eng. Sci. 19 441-51

[10] Solomon G M and Schettler T 2000 Environmentand health: 6. Endocrine disruption and potential human health implications Cmaj 163 1471-6

[11] Cartinella J L, Cath T Y, Flynn M T, Miller G C, Hunter K W and Childress A E 2006 Removal of natural steroid hormones from wastewater using membrane contactor processes Environ. Sci. Technol. 40 7381-6

[12] Johnson AC et al 2005 Comparing steroid estrogen and nonylphenol content across a range of European sewage plants with different treatment and management practices Water Res. 39 47-58

[13] Sarmah A K, Northcott G L, Leusch F D L and Tremblay L A 2006 A survey of endocrine disrupting chemicals (EDCs) in municipal sewage and animal waste effluents in the Waikato region of New Zealand Sci. Total Environ. 355 135-44

[14] Vymazal J, Březinová T and Koželuh M 2015 Occurrence and removal of estrogens, progesterone and testosterone in three constructed wetlands treating municipal sewage in the Czech Republic Sci. Total Environ. 536 625-31

[15] Han J, Qiu W, Cao Z, Hu J and Gao W 2013 Adsorption of ethinylestradiol (EE2) on polyamide 612: molecular modeling and effects of water chemistry Water Res. 47 2273-84

16] Braga O, Smythe G A, Schafer A I and Feitz A J 2005 Fate of steroid estrogens in Australian inland and coastal wastewater treatment plants Environ. Sci. Technol. 39 3351-8

[17] Limpiyakorn T, Homklin S and Ong S K 2011 Fate of estrogens and estrogenic potentials in sewerage systems Crit. Rev. Environ. Sci. Technol. 41 1231-70

[18] Aris A Z, Shamsuddin A S and Praveena S M 2014 Occurrence of 17a-ethynylestradiol (EE2) in the environment and effect on exposed biota: a review Environ. Int. 69 104-19

[19] Adeel M, Song X, Wang Y, Francis D and Yang Y 2017 Environmental impact of estrogens on human, animal and plant life: a critical review Environ. Int. 99 107-19

[20] Siegenthaler P F, Bain P, Riva F and Fent K 2017 Effects of antiandrogenic progestins, chlormadinone and cyproterone acetate and the estrogen 17a-ethinylestradiol (EE2) and their mixtures: transactivation with human and rainbowfish hormone receptors and transcriptional effects in zebrafish (Danio rerio) Aquatic Toxicol. 182 142-62

[21] Semiao A J C and Schafer A I 2010 Xenobiotics removal by membrane technology: an overview Xenobiotics in the Urban Water Cycle (Environmental Pollution) ed D Fatta-Kassinos, K Bester and K Kummerer vol 16 (Dordrecht: Springer) 307-38

[22] Luo Y, Guo W, Ngo H H, Nghiem L D, Hai F I, Zhang J, Liang S and Wang X C 2014 A review on the occurrence of micropollutants in the aquatic environment and their fate and removal during wastewater treatment Sci. Total Environ. 473-474 619-41

[23] Tijani J O, Fatoba O O and Petrik L F 2013 A review of pharmaceuticals and endocrine-disrupting compounds: sources, effects, removal and detections Water Air Soil Pollut. 224 1770

[24] Onesios K M, Yu J T and Bouwer E J 2009 Biodegradation and removal of pharmaceuticals and personal care products in treatment systems: a review Biodegradation. 20 441-66

[25] Pham T T, Nguyen V A and Van der Bruggen B 2013 Pilot scale evaluation of gac adsorption using low-cost, high-performance materials for removal of pesticides and organic matter in drinking water production J. Environ. Eng. 139 958-65

[26] Ali H, Masar M, Urbanek M, Guler A C, Urbanek P, Machovsky M and Kuritka I 2020 Effect of annealing on luminescence and photocatalytic activity of ZnS nanocrystals under UV light irradiation NANOCON 2020 Conf. Proc. pp 261-6

[27] Pendergast M M and Hoek E M V 2011 A review of water treatment membrane nanotechnologies Energy Environ. Sci. 4 1946-71

[28] Shannon M A, Bohn P W, Elimelech M, Georgiadis J G, Maňas B J and Mayes A M 2008 Science and technology for water purification in the coming decades Nature 452 301-10

[29] Kumar A K and Mohan S V 2011 Endocrine disruptive synthetic estrogen (17a-ethynylestradiol) removal from aqueous phase through batch and column sorption studies: Mechanistic and kinetic analysis Desalination 276 66-74

[30] Kumar A K, Mohan S V and Sarma P N 2009 Sorptive removal of endocrine-disruptive compound (estriol, E3) from aqueous phase by batch and column studies: kinetic and mechanistic evaluation J. Hazard. Mater. 164 820-8

[31] Pan B, Lin D, Mashayekhi H and Xing B 2008 Adsorption and hysteresis of bisphenol A and 17a-ethinyl estradiol on carbon nanomaterials Environ. Sci. Technol. 42 5480-5

[32] Jin X, Hu J Y, Tint M L, Ong S L, Biryulin Y and Polotskaya G 2007 Estrogenic compounds removal by fullerene-containing membranes Desalination 214 83-90

[33] Kiran Kumar A and Venkata Mohan S 2012 Removal of natural and synthetic endocrine disrupting estrogens by multi-walled carbon nanotubes (MWCNT) as adsorbent: kinetic and mechanistic evaluation Sep. Purif. Technol. 87 22-30

[34] Krupadam R J, Sridevi P and Sakunthala S 2011 Removal of endocrine disrupting chemicals from contaminated industrial groundwater using chitin as a biosorbent J. Chem. Technol. Biotechnol. 86 367-74

[35] Zhang Y and Zhou J L 2005 Removal of estrone and 17/β- estradiol from water by adsorption Water Res. 3991-4003

[36] Hristovski K D, Nguyen H and Westerhoff P K 2009 Removal of arsenate and 17a-ethinyl estradiol (EE2) by iron (hydr) oxide modified activated carbon fibers J. Environ. Sci. Heal. A 44 354-61

[37] Wang J, Pan K, Giannelis E P and Cao B 2013 Polyacrylonitrile/polyaniline core/shell nanofiber mat for removal of hexavalent chromium from aqueous solution: mechanism and applications RSC Adv. 3 8978-87

[38] Augusto F, Hantao L W, Mogollón N G S and Braga S C G N 2013 New materials and trends in sorbents for solid-phase extraction TrAC Trends Anal. Chem. 43 14-23

[39] Bhardwaj N and Kundu S C 2010 Electrospinning: a fascinating fiber fabrication technique Biotechnol. Adv. 28 325-47

[40] Yang Z, Peng H, Wang W and Liu T 2010 Crystallization behavior of poly(e-caprolactone)/layered double hydroxide nanocomposites J. Appl. Polym. Sci. 116 2658-67

[41] Yudanova T N, Filatov I Y and Afanasov IM 2016 Production of ultrafine cellulose acetate fibers Theor. Found. Chem. Eng. 50 508-12

[42] Dzenis Y 2004 Spinning continuous fibers for nanotechnology Science 304 1917-9

[43] Shabafrooz V, Mozafari M, Vashaee D and Tayebi L 2014 Electrospun nanofibers: from filtration membranes to highly specialized tissue engineering scaffolds J. Nanosci. Nanotechnol. 14 522-34

[44] Hemamalini T, Karunakaran S A, Siva Elango M K, Senthil Ram T and Giri Dev V R 2019 Regeneration of cellulose acetate nanofibrous mat from discarded cigarette butts Indian J. Fibre Text. Res. 44 248-52

[45] Kimmer D, Vincent I, Lovecka L, Kazda T, Giurg A and Skorvan O 2017 Some aspects of applying nanostructured materials in air filtration, water filtration and electrical engineering AIP Conf. Proc. 1843 060001

[46] Chigome S and Torto N 2011 A review of opportunities for electrospun nanofibers in analytical chemistry Anal. Chim. Acta 706 25-36

[47] Chigome S, Darko G and Torto N 2011 Electrospun nanofibers as sorbent material for solid phase extraction Analyst 136 2879-89

[48] Niavarani Z, Breite D, Prager A, Abel B and Schulze A 2021 Estradiol removal by adsorptive coating of a microfiltration membrane Membranes 11 1-13

[49] Wang M, Qu F, Jia R, Sun S, Li G and Liang H 2016 Preliminary study on the removal of steroidal estrogens using TiO2-doped PVDF ultrafiltration membranes Water 8 1 -12

[50] Kimmer D, Vincent I, Fenyk J, Petras D, Zatloukal M, Sambaer W and Zdimal V 2011 Morphology of nano and micro fiber structures in ultrafine particles filtration AIP Conf Proc. 1375 295-311

[51] Szewczyk P K, Ura D P, Metwally S, Knapczyk-Korczak J, Gajek M, Marzec M M, Bernasik A and Stachewicz U 2018 Roughness and fiber fraction dominated wetting of electrospun fiber-based porous meshes Polymers 11 34

[52] Yasir M, Sopík T, Kimmer D and Sedlařík V 2021 Facile hplc technique for simultaneous detection of estrogentic hormones in wastewater Nanocon Conf. Proc.—Int. Conf. Nanomater (2021 October 2021), pp 272-6

[53] Qi F F, Cao Y, Wang M, Rong F and Xu Q 2014 Nylon 6 electrospun nanofibers mat as effective sorbent for the removal of estrogens: kinetic and thermodynamic studies Nanoscale Res. Lett. 9 1-10

[54] Al-Khateeb L A, Obaid A Y, Asiri N A and Abdel Salam M 2014 Adsorption behavior of estrogenic compounds on carbon nanotubes from aqueous solutions: kinetic and thermodynamic studies J. Ind. Eng. Chem. 20 916-24

[55] Taha A A, Na Wu Y, Wang H and Li F 2012 Preparationandapplication of functionalized cellulose acetate/silica compositenanofibrous membrane via electrospinning for Cr(VI) ion removal from aqueoussolution J. Environ. Manage. 112 10-6

[56] Tian Y, Wu M, Liu R, Li Y, Wang D, Tan J, Wu R and Huang Y 2011 Electrospun membrane of cellulose acetate for heavy metal ion adsorption in water treatment Carbohydrate Polym. 83 743-8

[57] Celebioglu A, Demirci S and Uyar T 2014 Cyclodextrin- grafted electrospun cellulose acetate nanofibers via 'click' reaction for removal of phenanthrene Appl. Surf. Sci. 305 581-8

[58] Mikaeili F and Gouma P I 2018 Super water-repellent cellulose acetate mats Sci. Rep. 8 1 -8

[59] Karbownik I, Rac-Rumijowska O, Fiedot-Toboła M, Rybicki T and Teterycz H 2019 The preparation and characterization of polyacrylonitrile-polyaniline (PAN/ PANI) fibers Materials 12 664

[60] Han X J, Cheng B J, Li Y J, Huang Z M, Huang C, Du Z F and Wang J 2015 The effects of electrospinning parameters on coaxial polyacrylonitrile/polyurethane nanofibers: morphology and water vapour transmission rate Fibers Polym. 16 2237-43

[61] Sundaran S P, Reshmi C R and Sujith A 2018 Tailored design of polyurethane based fouling-tolerant nanofibrous membrane for water treatment New J. Chem. 42 1958-72

[62] Kwak N S, Jung W H, Park H M and Hwang T S 2013 Electrospun polyethersulfone fibrous mats: sulfonation, its characterization and solution-phase ammonium sorption behavior Chem. Eng. J. 215-216 375-82

[63] Xu Y, Bao J, Zhang X, Li W, Xie Y, Sun S, Zhao W and Zhao C 2019 Functionalized polyethersulfone nanofibrous membranes with ultra-high adsorption capacity for organic dyes by one-step electrospinning J. Colloid Interface Sci. 533 526-38

[64] Han J, Qiu W, Hu J and Gao W 2012 Chemisorption of estrone in nylon microfiltration membranes: adsorption mechanism and potential use for estrone removal from water Water Res. 46 873-81

[65] Benavente M J, Caballero M J A, Silvero G, López-Coca I and Escobar V G 2019 Cellulose acetate recovery from cigarette butts Proceedings. 2 1447

[66] Nasir M, Subhan A, Prihandoko B and Lestariningsih T 2017 Nanostructure and property of electrospun sio2-cellulose acetate nanofiber composite by electrospinning Energy Proc. 107 227-31

[67] Vazquez-Velez E, Lopez-Zarate L and Martinez-Valencia H 2020 Electrospinning of polyacrylonitrile nanofibers embedded with zerovalent iron and cerium oxide nanoparticles, as Cr(VI) adsorbents for water treatment J. Appl. Polym. Sci. 137 1-10

[68] Luo Z, Li H, Yang Y, Lin H and Yang Z 2017 Adsorption of 17a-ethinylestradiol from aqueous solution onto a reduced graphene oxide-magnetic composite J. Taiwan Inst. Chem. Eng. 80 797-804

[69] Gunay A, Arslankaya E and Tosun I 2007 Lead removal from aqueous solution by natural and pretreated clinoptilolite: adsorption equilibrium and kinetics J. Hazard. Mater. 146 362-71

[70] Ersali S, Hadadi V, Moradi O and Fakhri A 2013 Pseudo- second-order kinetic equations for modeling adsorption systems for removal of ammonium ions using multi-walled carbon nanotube Fullerenes, Nanotube Carbon Nanostructures 141217112133007

[71] Esmaeeli F, Gorbanian S A and Moazezi N 2017 Removal of estradiol valerate and progesterone using powdered and granular activated carbon from aqueous solutions Int. J. Environ. Res. 11 695-705

[72] He J, Zhou Q, Guo J and Fang F 2018 Characterization of potassium hydroxide modified anthracite particles and enhanced removal of 17a-ethinylestradiol and bisphenol A Environ. Sci. Pollut. Res. 25 22224-35

[73] Porter J J and Porter R S 1995 Filtration studies of selected anionic dyes using asymmetric titanium dioxide membranes on porous stainless-steel tubes J. Member Sci. 101 67-81

[74] Auriol M, Filali-Meknassi Y, Adams C D and Tyagi R D 2006 Natural and synthetic hormone removal using the horseradish peroxidase enzyme: temperature and pH effects Water Res. 40 2847-56

[75] Behera S K, Kim H W, Oh J E and Park H S 2011 Occurrence and removal of antibiotics, hormones and several other pharmaceuticals in wastewater treatment plants of the largest industrial city of Korea Sci. Total Environ. 409 4351-60

[76] Bayode A A et al 2021 Carbon-mediated visible-light clay-Fe2O3-graphene oxide catalytic nanocomposites for the removal of steroid estrogens from water J. Water Proc. Eng. 40 101865

[77] Pinto A M, Moreira S, Gonęalves I C, Gama F M, Mendes A M and Magalhaes F D 2013 Biocompatibility of poly(lactic acid) with incorporated graphene-based materials Colloids Surf B 104 229-38